June 2004 Update to the NOνA (P-929) Proposal

Rev 06/15/04

Appendix D.
Update on the Physics Potential of NOνA

D.1. Introduction

This appendix is written in response to the PAC's request for "a revised proposal … covering (1) how NOνA extends the understanding of phenomena in the neutrino sector in the context of other planned experiments, and (2) how the initial experimental setup can smoothly evolve in conjunction with a proton driver for future measurements of mass hierarchy and CP violation." This appendix will address the major PAC questions. Detailed questions not covered here will be addressed in the oral presentation.

Provided that θ_{13} is in the range accessible to conventional neutrino beams, the unique contribution of the NuMI neutrino program will be the resolution of the mass hierarchy. This can only be done by experiments that measure the matter effect due to ν_e's traveling long distances through the earth. Planned future experiments in both Japan [1] and Europe [2] are concentrating on baselines that are too short for this purpose.

The determination of whether the solar neutrino doublet is at a higher or lower mass than the third neutrino mass state is important in its own right, for interpreting neutrinoless double beta decay experiments, and for the eventual measurement of CP violation in the lepton sector. As an example of the last, consider Fig. D.1, which is taken from the T2K LoI [1]. The T2K collaboration is proposing a very ambitious long-term program to make precision measurements of CP violation by increasing the JPARC proton intensity by a factor of 5 (to 4 MW) and by building a new detector, HyperKamiokande, which will have twenty times the mass of SuperKamiokande. Fig. D.1. shows the numbers of ν_e and $\bar{\nu}_e$ appearance events with two years of neutrino and six years of antineutrino running for $\sin^2(2\theta_{13}) = 0.1$. It is clear that without a resolution of the mass hierarchy, there are large areas of the parameter space in which the CP

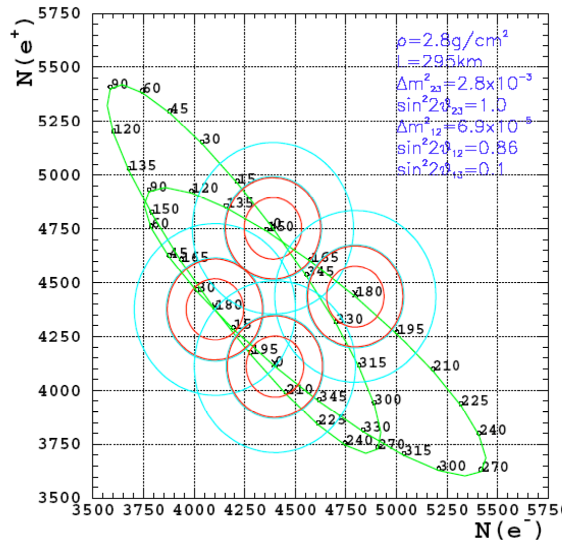

Fig. D.1: The numbers of ν_e and $\bar{\nu}_e$ appearance events with two years of neutrino and six years of antineutrino running for $\sin^2(2\theta_{13}) = 0.1$ in an anticipated experiment utilizing an upgraded JPARC proton beam and the HyperKamiokande detector. Each of the two green contours corresponds to the different mass hierarchy and the numbers on the contours are the CP phase in degrees. The red circles correspond to the 90% confidence level contours and the blue circles correspond to three standard deviation contours. The outer circles include errors due to a 2% systematic uncertainty. From the T2K LoI [1].

phase cannot be determined with any precision. The JPARC program is relying on the NuMI program for this information. This will be made quantitative in Section D.5 of this appendix. Given this unique role for the NOνA experiment, we believe it should be designed and sited to optimize this role. There are two aspects of this problem. The first is illustrated in Fig. D.2, which shows all of the values of the parameters consistent with a (perfectly measured) 2% $\nu_\mu \rightarrow \nu_e$ oscillation probability 12 km off axis at an 810 km baseline. There are three parameters, $\sin^2(2\theta_{13})$, shown on the vertical axis, the two possible mass orderings, the normal hierarchy, shown by the solid blue curve and the inverted hierarchy, shown by the dashed red curve, and the CP phase δ, shown as values around the ellipses. The horizontal axis shows the result of a (perfect) measurement of the $\bar{\nu}_\mu \to \bar{\nu}_e$ oscillation probability.[1]

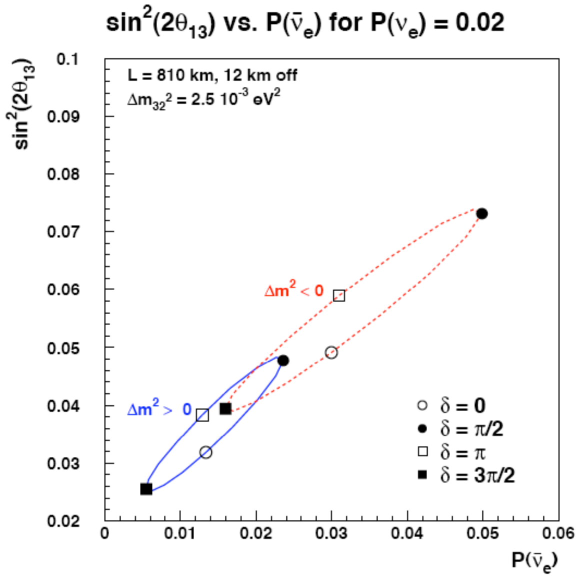

Fig. D.2: Plot of the possible results of a measurement of a 2% neutrino oscillation probability. See text for an explanation.

NOνA is capable of making two measurements, the neutrino and the antineutrino oscillation probabilities near the first oscillation maximum. In some cases, these two measurements are capable, in principle, of measuring all three parameters, up to a two-fold ambiguity in the CP phase. For example a neutrino oscillation probability of 2% and an antineutrino oscillation probability of 4% or 1%, determine the mass hierarchy unambiguously. However, a neutrino oscillation probability of 2% and an antineutrino oscillation probability of 2% cannot resolve the inherent ambiguity shown in Fig. D.2. A third measurement is needed in this case, either from an experiment done elsewhere at a different baseline, or from an additional measurement on the NuMI beamline, for example, on the second oscillation maximum.

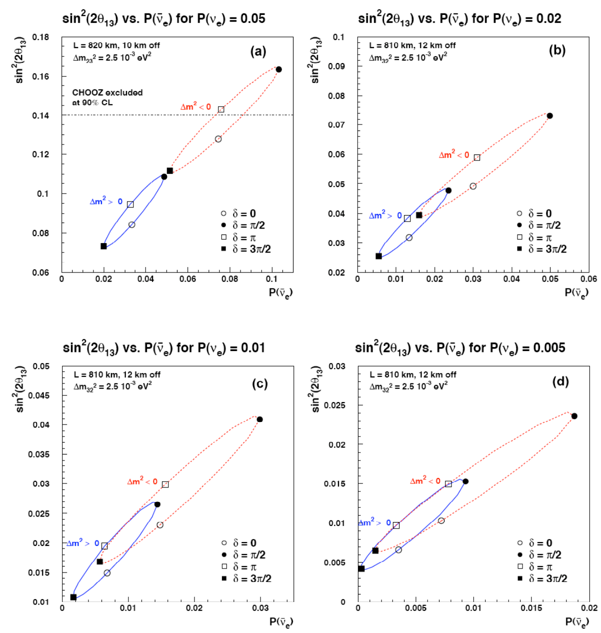

Fig. D.3: Plots of the possible results of a measurement of a (a) 5%, (b) 2%, (c) 1%, and (d) 0.5% neutrino oscillation probability. See text for an explanation.

Figure D.3 shows the same information as Fig. D.2, except for neutrino oscillation probabilities of 0.5%, 1%, 2% (again), and 5%. This figure illustrates that the fraction of possible δ values for which there is an ambiguity increases with decreasing values of θ_{13}.

The second aspect of the optimization problem is illustrated in Fig. D.4. The figure of merit (FoM) squared and the neutrino asymmetry are plotted as a function of the off-axis transverse angle for $\Delta m^2_{32} = 0.0025\ \mathrm{eV}^2$. The FoM is defined as the signal divided by the square root of the back-

[1] Figs. D.2 and D.3 are drawn assuming that $\sin^2(2\theta_{23})$ = 1.0. If it is less than unity, then there will be a two-fold ambiguity in the value of $\sin^2(2\theta_{13})$ derived from $\nu_\mu \to \nu_e$ oscillations since the "atmospheric scale" oscillation probability is proportional to $\sin^2(\theta_{23})$. Since this factor is the same for all $\nu_\mu \to \nu_e$ oscillation experiments, it will not affect the resolution of the mass hierarchy or the determinations of the CP-violating phase δ by these experiments. It will, however, affect the comparison of these experiments to reactor experiments, and may eventually be resolved by the comparison of precise reactor and accelerator oscillation experiments.

ground. It is proportional to the sensitivity (in standard deviations) for seeing an oscillation signal, and the inverse of its square is proportional to amount of detector mass times beam flux required to obtain a given result. The neutrino asymmetry is defined as the neutrino oscillation probability minus the antineutrino probability divided by their sum, due to the matter effect. Thus, it is a measure of how far the two ellipses separate in Figs. D.2 and D.3. The ability to resolve the mass hierarchy will depend on both the rate of events as given by the FoM and separation given by neutrino asymmetry.

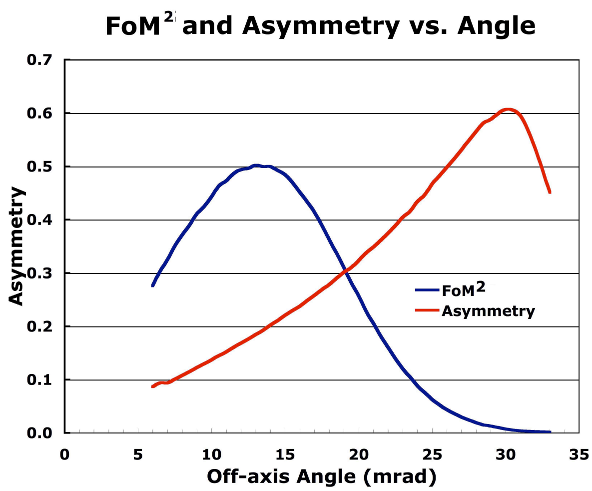

Fig. D.4: Figure of merit squared (arbitrary units) and neutrino oscillation asymmetry due to the matter effect for $\Delta m^2 = 0.0025$ eV^2 versus off-axis angle. See text for an explanation. This figure is for illustrative purposes. It is based on a toy model and may not agree precisely with the simulation data presented in this appendix.

Figure D.4 shows that the sensitivity to observing the oscillation will not optimize at the same place as the sensitivity to the mass hierarchy. However, in this appendix we will show that optimizing for resolving the mass hierarchy results in only a small loss of sensitivity for seeing the oscillation. Further, this optimization will be correct for each possible future stage of the evolution of the NOνA program, and it is insensitive to the value of Δm^2_{32} within the range suggested by the latest SuperKamiokande analysis.[2]

The conclusion of this appendix will be that NOνA is optimized for a long-range program that is capable of resolving the mass hierarchy over most of the range accessible to conventional neutrino beams. In addition, we will show that with the construction of a Proton Driver at Fermilab, NOνA will have a substantial capability to measure CP violation, both alone and in combination with other experiments.

D.2. Simulations

In preparation for addressing the PAC questions, we have redone all of our simulations using the techniques described in Chapter 8. Two minor, partially canceling bugs were corrected. There was an error in the fiducial containment and a miscommunication about how much flux the calculations were being done for. There was also a bush-league statistics error in the calculation of Fig. 5.5, which underestimated the NOνA potential, and which was caught by a sharp-eyed member of the PAC.

The simulations were made for 6, 8, 10, 12, 14, and 16 km off-axis transverse distance for Δm^2_{32} = 0.0025 eV^2 and for 8, 10, 12, and 14 km for Δm^2_{32} = 0.0020 eV^2. The simulations were optimized separately for each set of parameters. The results presented here supersede those presented in Chapters 5 and 8.

Table D.1 gives the results of the simulations for 5 years of running at 4×10^{20} pot/yr into the NOνA detector at a baseline of 810 km. The signal is the number of observed events without any matter or CP effects; that is, in the language of Chapter 3, it corresponds to $\frac{1}{2}\sin^2(2\theta_{13})\sin^2\Delta_{31}$, assuming $\sin^2(2\theta_{13}) = 0.1$. The background includes both neutrino and antineutrino backgrounds.

[2] An analysis presented at the NOON2004 conference gives a best fit at $\Delta m^2_{23} = 0.0024$ eV^2 and a 90% confidence level lower limit of 0.0019 eV^2. [3]

Offset (km)	Type	Δm^2 (10^{-3} eV^2)	Signal	Back-ground	FoM
6	ν	2.5	237	83	26.0
8	ν	2.5	205	52	28.4
10	ν	2.5	158	33	27.5
12	ν	2.5	125	26	24.5
14	ν	2.5	85	19	19.5
16	ν	2.5	51	14	13.6
6	$\bar{\nu}$	2.5	167	77	19.0
8	$\bar{\nu}$	2.5	137	50	19.4
10	$\bar{\nu}$	2.5	98	30	17.9
12	$\bar{\nu}$	2.5	69	26	13.5
14	$\bar{\nu}$	2.5	38	15	9.8
16	$\bar{\nu}$	2.5	22	13	6.1
8	ν	2.0	149	53	20.5
10	ν	2.0	120	34	20.6
12	ν	2.0	101	27	19.4
14	ν	2.0	75	19	17.2
8	$\bar{\nu}$	2.0	99	51	13.9
10	$\bar{\nu}$	2.0	75	31	13.5
12	$\bar{\nu}$	2.0	52	22	11.1
14	$\bar{\nu}$	2.0	33	15	8.5

Table D.1: Simulation results for 5 years of running at 4×10^{20} pot/yr into the NOνA detector at a baseline of 810 km, assuming that $\sin^2(2\theta_{13}) = 0.1$, and without solar, matter, or CP contributions.

D.3. Sensitivity to Observing $\nu_\mu \to \nu_e$ Oscillations

Figures D.4 and D.5 show the calculated three standard deviation discovery limit for $\nu_\mu \to \nu_e$ oscillations in terms of the three unknown parameters, assuming $\Delta m^2_{32} = 0.0025$ eV^2. The vertical axis represents the fraction of possible δ values for which a 3-σ discovery could be made. In other words, zero represents the limit for the most favorable value of δ for a given $\sin^2(2\theta_{13})$, one represents the least favorable value of δ, and 0.5 represents a typical value. The curves represent the two possible values of the sign of Δm^2_{32} and different assumptions on the number of protons on target (pot) that the experiment might see in a five-year run. (If these figures are being viewed in gray scale, the line to the right for each number of protons represents the inverted mass hierarchy.)

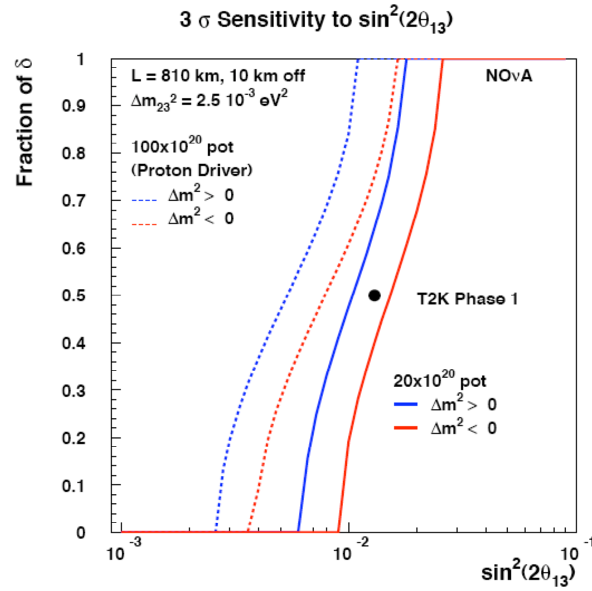

Figure D.4: Three standard deviation discovery limits for the observation of $\nu_\mu \to \nu_e$ oscillations for the NOνA detector situated 10 km off the NuMI beamline. See the text for more details.

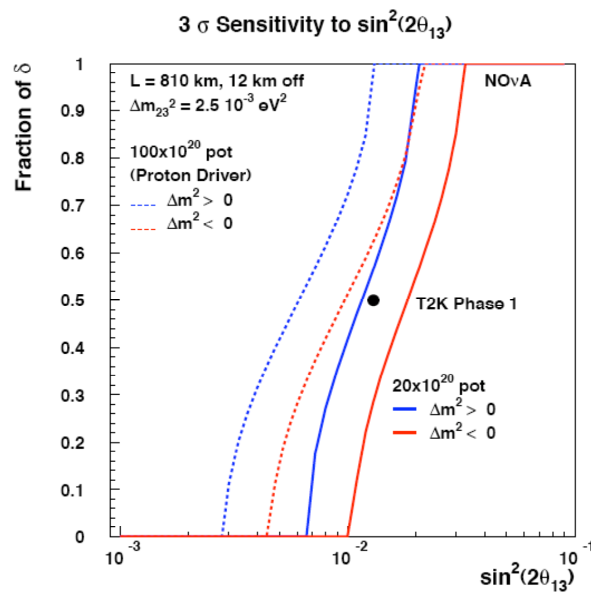

Figure D.5: Three standard deviation discovery limits for the observation of $\nu_\mu \to \nu_e$ oscillations for the NOνA detector situated 12 km off the NuMI beamline. See the text for more details.

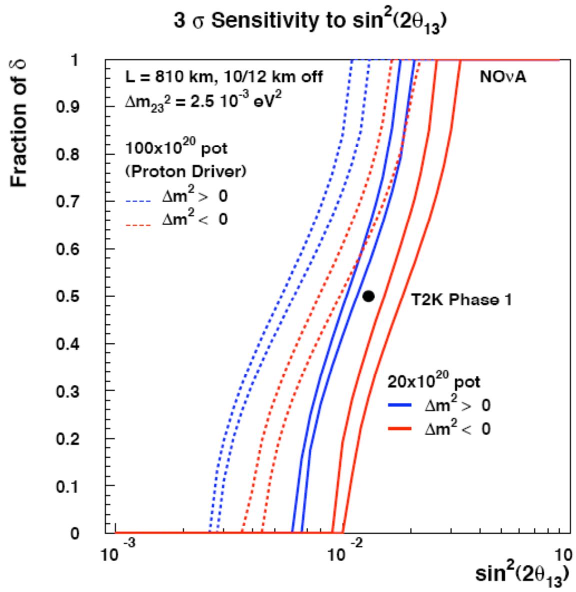

Figure D.6: Data from Figs. D.4 and D.5 superimposed for comparison purposes.

The value of 20×10^{20} pot represents our estimate of what Fermilab might be able to deliver in a five-year run with incremental Booster and Main Injector improvements, while 100×10^{20} pot represents the expectation with the Booster replaced by a new Proton Driver. A 5% systematic error on the background determination has been included in these and the other calculations presented in this appendix, but as can be seen from Table D.1, the statistical errors on the backgrounds always dominate. The three standard deviation sensitivity of the T2K phase 1 proposal [1] is also shown in these figures.

Figures D.4 and D.5 differ in that the former displays data for the NOνA detector situated 10 km off-axis, while the later is for 12 km off-axis. There is some loss of sensitivity in going from 10 to 12 km. This is best seen in Fig. D.6, which superimposes the data from the previous two figures. There is only a minor loss of sensitivity for the normal mass hierarchy, because the larger matter effects at 12 km enhance the neutrino oscillation probability. The loss is somewhat larger, but still relatively small, for the inverted mass hierarchy, where the matter effects suppress the neutrino oscillation probability.

Figure D.7 shows the three standard deviation discovery limits for the typical δ for all of the cases listed in Table D.1. For all cases, the sensitivity maximizes at 8 km off-axis, with the exception of the point at Δm^2_{32} = 0.0025 eV^2, inverted mass hierarchy, where it is slightly better at 6 km. Figure D.7 also shows the loss of sensitivity going from Δm^2_{32} = 0.0025 eV^2 to Δm^2_{32} = 0.0020 eV^2. However, it should be noted that this is not a loss in range, since the CHOOZ limit [4] is correspondingly weaker at 0.0020 eV^2.

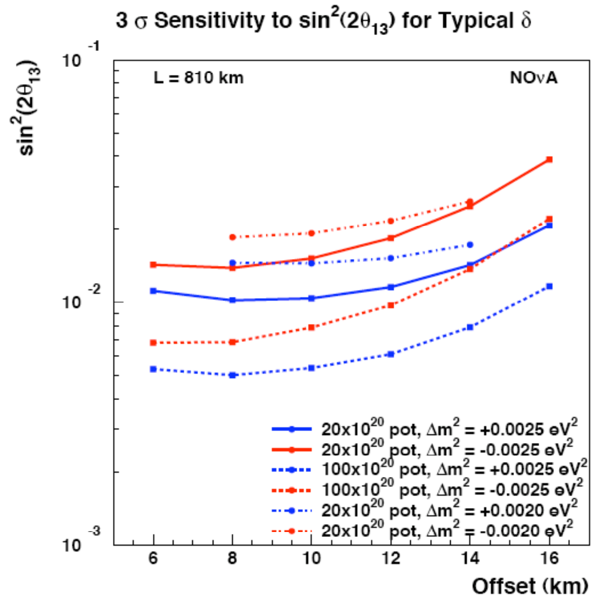

Figure D.7: Three standard deviation discovery limits for the observation of $\nu_\mu \rightarrow \nu_e$ oscillations for the typical CP phase δ versus the NOνA detector off-axis distance for the integrated fluxes and Δm^2 values shown.

One of the PAC questions asked about the worst possible scenario. Given the recent SuperKamiokande result [3], we tend to consider Δm^2_{32} = 0.0020 eV^2 as a reasonable estimate for the worst possible scenario.

D.4. Sensitivity to the Mass Hierarchy

D.4.1. NOνA Alone: Figure D.8 shows the 95% confidence level resolution of the mass hierarchy as a function of $\sin^2(2\theta_{13})$ for the NOνA detector sited a 12 km off-axis. The 95% confidence level has been chosen since the mass hierarchy is binary, so 20:1 odds should be reasonably convincing. The assumed scenario is that within three years of neutrino running, a three-σ signal is observed for ν_e appearance, after which the running is switched to antineutrinos for studying the mass hierarchy. Thus, Fig. D.8 assumes three years of each neutrino and antineutrino running, both with and without a proton driver.

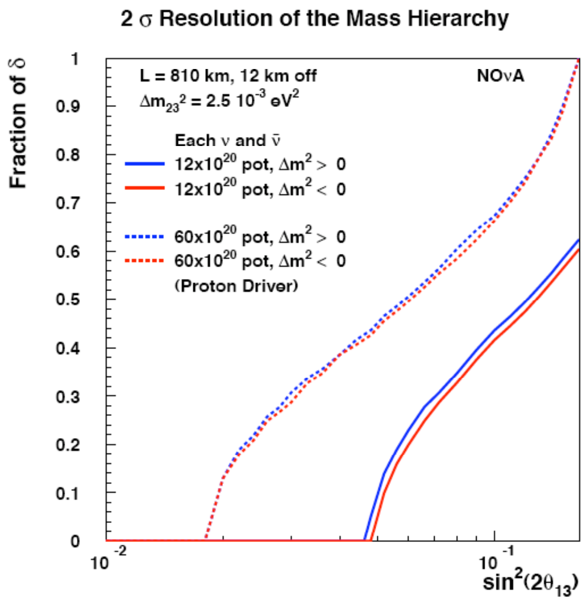

Figure D.8: The 95% confidence level resolution of the mass hierarchy versus $\sin^2(2\theta_{13})$ for three years of running each neutrinos and antineutrinos, with and without a proton driver.

The shapes of the curves are easily understood from Fig. D.3. There is a limited range of δ values for which two measurements can resolve the mass hierarchy, and this range decreases with decreasing values of $\sin^2(2\theta_{13})$. There is a reasonable region of parameter space in which NOνA could resolve the mass hierarchy before a Proton Driver is available, and a considerably larger region after.

To emphasize the point that only a long baseline experiment can resolve the mass hierarchy, we have calculated the sensitivity of T2K phase 1, if it were to run for three years each on neutrinos and antineutrinos. This is shown in Fig. D.9. The horizontal scale has been expanded in order to show the T2K sensitivity, which otherwise would be off-scale to the right. The CHOOZ limit for $\Delta m^2_{32} = 0.0025\ \mathrm{eV}^2$ is also indicated [4]. Points substantially to the right of this limit are largely irrelevant. We emphasize that the results for T2K are our calculations, since the T2K collaboration, quite sensibly, has not proposed this measurement.

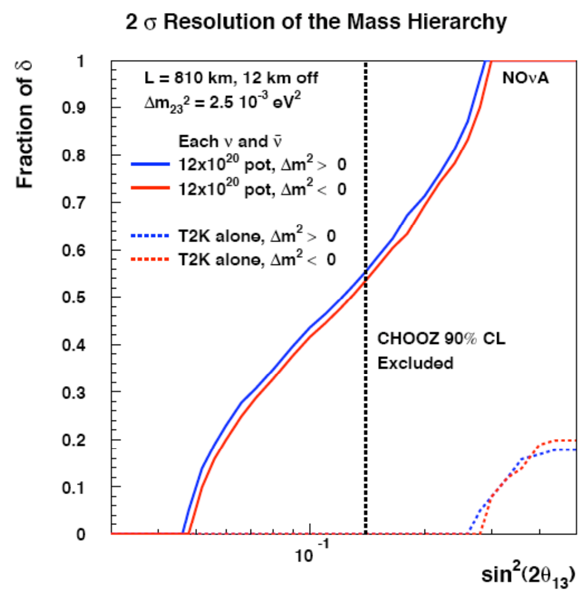

Fig. D.9: A comparison of NOνA's and T2K's abilities to resolve the mass hierarchy alone.

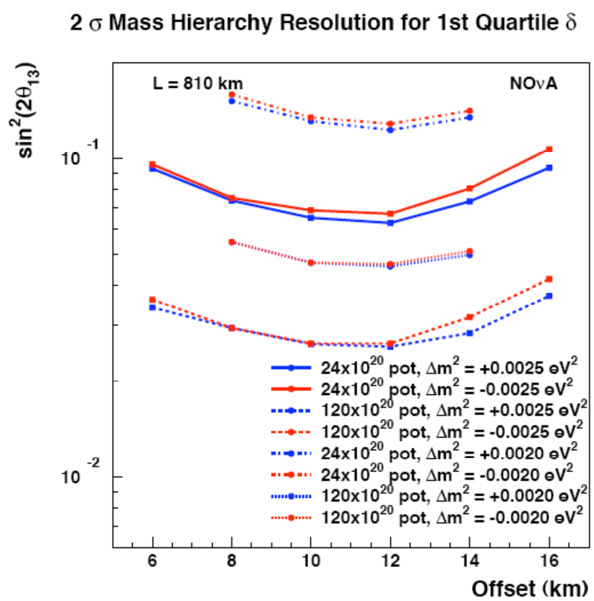

Fig. D.10: 95% confidence level for resolution of the mass hierarchy for the 1st quartile δ. See the text for additional explanation.

Figure D.10 shows the mass hierarchy resolution sensitivity for all of the simulations in Table D.1. This figure displays the value of $\sin^2(2\theta_{13})$ for which the δ value is at the limit of first quartile, i.e., the δ value such that 25% of δ values give a lower value of $\sin^2(2\theta_{13})$ and 75% give a higher value. This δ was chosen because the typical δ is in the region of the CHOOZ limit for running before the Proton Driver, and thus less relevant. However, the siting optimization does not depend significantly on which δ value is chosen.

Fig. D.10 shows that the mass hierarchy resolution is optimum at 12 km off-axis for both Δm^2_{32} = 0.0025 and 0.0020 eV^2.

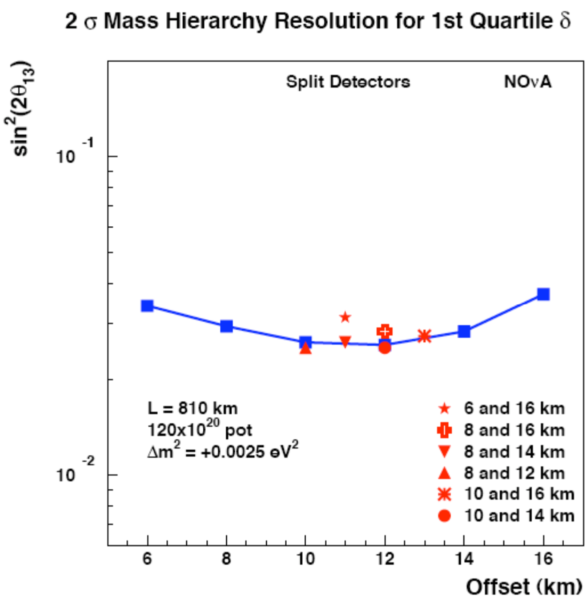

Fig. D.11: Comparison of the mass hierarchy resolution sensitivity between single detector sites and pairs of detector sites. See the text for details.

D.4.2Multiple Detector Sites: One question the PAC asked was whether better sensitivities could be obtained by having, say, half of the detector at each of two separated sites. The results of simulating this suggestion are shown in Fig. D.11 for six choices of pairs of detector sites. For clarity of presentation, only results for the normal mass hierarchy and for running with the Proton Driver are shown. The calculations were made without consideration of the loss of fiducial volume or the additional infrastructure that would be required.

Figure D.11 shows that there is indeed a gain, in principle, in dividing the detector in two. For example, splitting the detector between 6 and 16 km off-axis gives a result that is more sensitive than a single detector at either distance. Two cases are very slightly better than a single detector at 12 km off-axis, half detectors at 8 and 12 km, and half detectors at 10 and 14 km. However, the gain is only in the third significant digit and this would clearly not overcome the fiducial volume loss and the cost of the extra infrastructure.

It should be noted that if the TASD option is adopted, the energy resolution will be narrower than the width of the beam (see Section B.10.2), which gives the advantage of split detectors without the drawbacks. This will improve the performance for mass hierarchy resolution, but probably not by much.

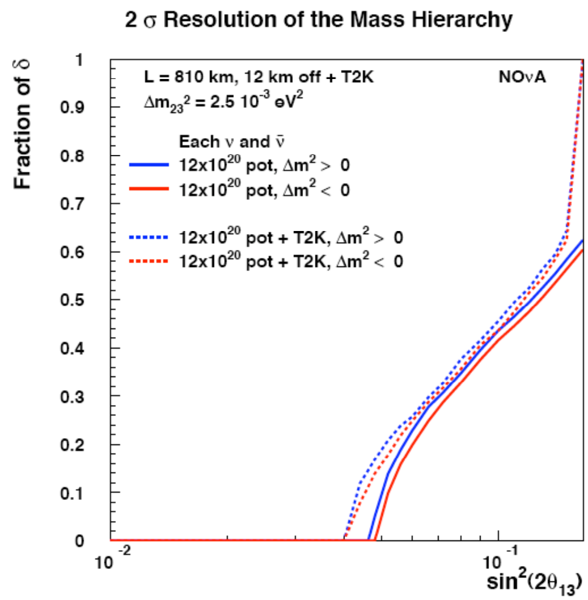

Fig. D.12: A comparison of the 95% confidence level resolution of the mass hierarchy with NOνA alone (solid curves) and the combination of NOνA and T2K phase 1 data (dashed curves). It is assumed that both NOνA and T2K run three years each on neutrinos and antineutrinos.

D.4.3: NOνA in Combination with Another Measurement: If the neutrino oscillation parameters are such that the mass hierarchy cannot be resolved by NOνA alone, then combining NOνA measurements with the measurement of another detector will be necessary. The most obvious candidate is T2K. Figures D.12 and D.13 show these results. Figure D.12 is for NOνA without the Proton Driver combined with T2K phase1. Figure D.13 is for a later time in which NOνA with the Proton Driver can be combined with T2K with an upgraded proton source. For this later case, we have calculated the results assuming either that the T2K detector is SuperKamiokande or HyperKamiokande.

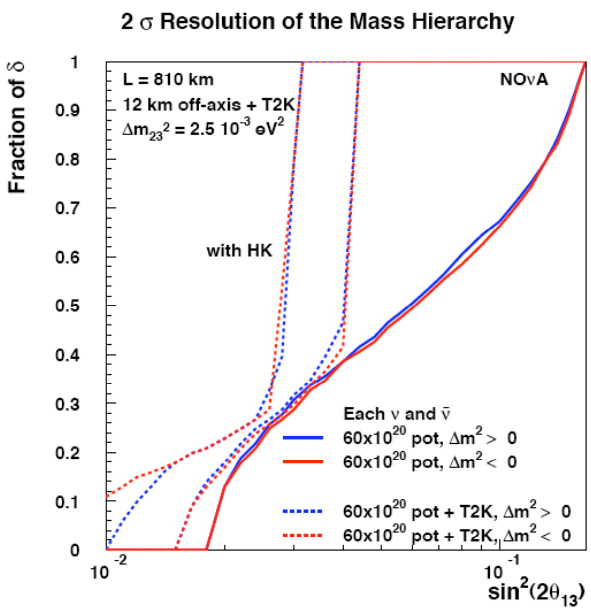

Fig. D.13: A comparison of the 95% confidence level resolution of the mass hierarchy with NOνA alone with the Proton Driver (solid curves) and the combination of NOνA and T2K data with an upgraded proton source (dashed curves). The curves labeled "HK" assume that the T2K detector is HyperKamiokande; the other set of dashed curves assume that it is SuperKamiokande. It is assumed that both NOνA and T2K run three years each on neutrinos and antineutrinos.

The structure of these plots is that the combination with T2K does not have much effect until a critical value of $\sin^2(2\theta_{13})$, after which the mass hierarchy is resolved for all values of δ. The reason for this is fairly easy to understand. We are comparing two distributions that have approximately the same structure due to the CP phase, and differ primarily by a factor of 2.3 in the matter effect. Thus, sufficient statistics to pass the 95% confidence level threshold happens for all values of δ at approximately the same point.

The difference between the critical value of $\sin^2(2\theta_{13})$ for HyperKamiokande is only about 30% lower than that for SuperKamiokande, even though the former has twenty times the mass of the latter. This is because the statistical precision is limited by the number of events in NOνA.

If comparisons with T2K are insufficient to resolve the mass hierarchy, then an attractive approach would be to do a measurement with an additional detector on the NuMI beamline to measure events at the second oscillation maximum. At the second maximum the matter effect is smaller by a factor of three and the CP violating effects are larger by a factor of three.

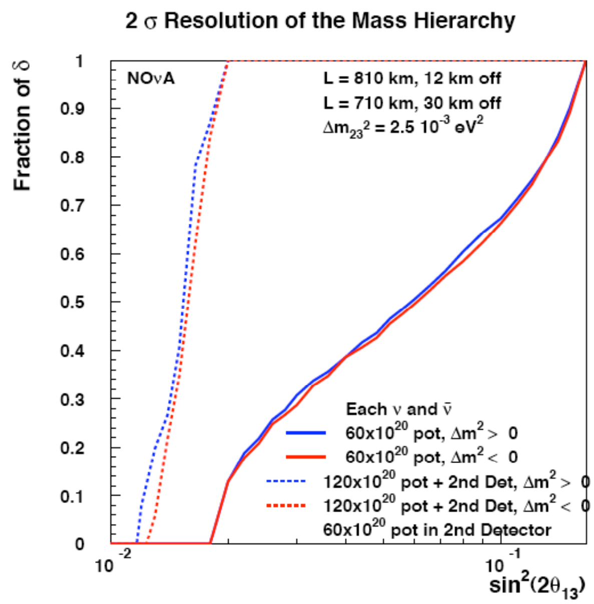

Fig. D.14: A comparison of the 95% confidence level resolution of the mass hierarchy with NOνA alone (solid curves) and the combination of NOνA and an additional NuMI detector sited to measure the second oscillation maximum (dashed curves). See the text for details of the scenario.

There will be sufficient information available at that time that it will be known whether this technique will work and how much detector mass will be required. For the purpose of our calculation, we have adopted the following scenario. After two years of running with the Proton Driver, it is realized that a second off-axis detector will be needed and it is constructed in four years and then runs for an additional six years. Thus, there will be twelve years of NOνA data with a Proton Driver and six years of data with the second detector, both split equally between neutrinos and antineutrinos. We have assumed that the second detector would have the same mass as NOνA for this illustration. The results are shown in Fig. D.14. The mass hierarchy is resolved for all values of δ for values of $\sin^2(2\theta_{13})$ greater than 0.01 to 0.02.

Fig. D.15 addresses the siting optimization for combinations of NOνA data with T2K data or with that of an additional NuMI detector. It displays the value of $\sin^2(2\theta_{13})$ at which the mass hierarchy is resolved at the 95% confidence level for all values of δ. Considering both mass hierarchies, 12 km is the optimum off-axis distance for the comparison with T2K, and 10 km is only very slightly more optimum than 12 km for comparison with a second off-axis NuMI detector. Thus, it appears that we can site NOνA at 12 km off-axis without fear that this decision will be non-optimal for later stages of the NuMI program. If the TASD option is adopted, we expect that the general conclusions of this appendix will not change, although TASD might optimize at slightly larger off-axis distances due to its better sensitivity to low-energy events.

D.4.4: Summary of the Evolution of the NOνA Program to Resolve the Mass Hierarchy: Figure D.16 summarizes the possible evolution of the NOνA program by combining the results shown in Figs. D.8, D.12, D.13, and D.14. The NOνA program allows the resolution of the mass hierarchy over most of the range in θ_{13} accessible to conventional neutrino beams. The program is flexible; each stage can be guided by the information obtained in prior stages, and the NOνA detector that we are proposing here remains a key and well-optimized participant throughout the program.

D.5. Sensitivity to CP Violation

D.5.1: Introduction: The relationship between the resolution of the mass hierarchy and the observation of CP violation varies from experiment to experiment. Very short baseline experiments, such as the beta beam experiments being planned in Europe [2] have very small matter effects and can measure CP violation phase δ without regard to the determination of the mass hierarchy. Long baseline experiments such as NOνA generally require a resolution of the mass hierarchy to measure the CP phase because maximal CP violation for one mass ordering can have the same or similar

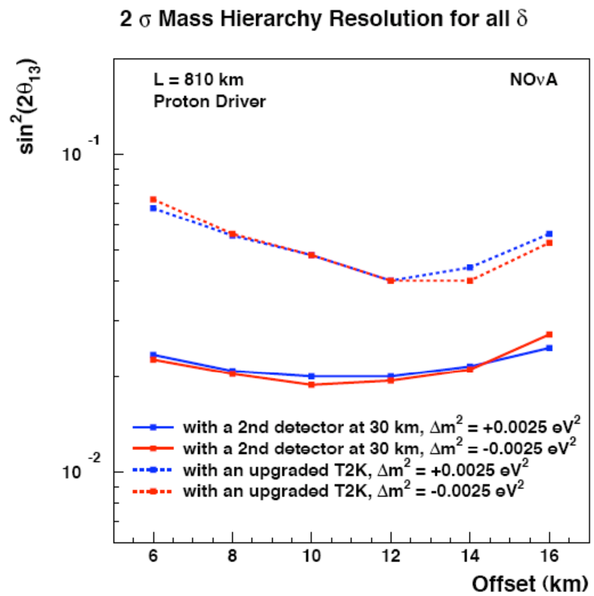

Fig. D.15: 95% confidence level for resolution of the mass hierarchy for all values of δ for various NOνA off-axis distances. The dashed lines are for a combination of NOνA data with the Proton Driver and T2K data with an upgraded proton source and SuperKamiokande as the T2K detector. The solid lines are for a combination of NOνA data with an additional NuMI detector as discussed in the text.

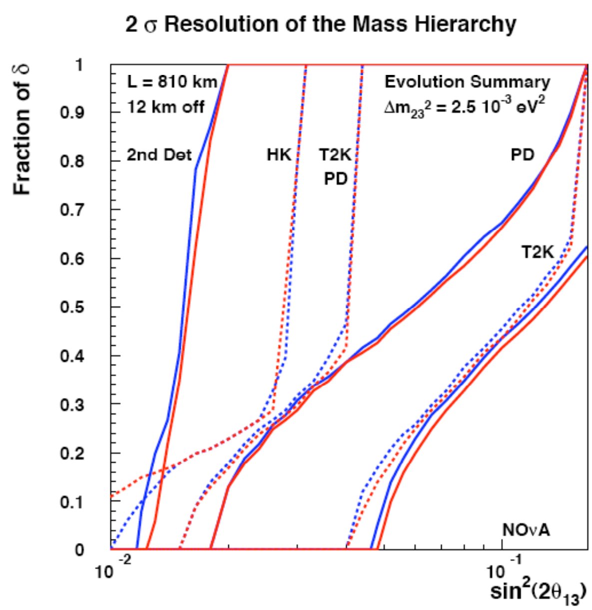

Fig. D.16: A summary of the data presented in Figs D.8, D.12, D.13, and D.14.

neutrino and antineutrino oscillation probabilities as no CP violation for the other mass ordering. An example of this is shown in Fig. D.3(c). Shorter baseline experiments such as T2K are intermediate between these extremes. This section will explore the capability of NOνA to measure the CP violating phase δ and the power of combinations of NOνA measurements with those of other experiments.

One should keep in mind that CP-violating effects are proportional to the first power of θ_{13}, while CP-conserving effects are, for the most part, proportional to the square of θ_{13}, as can be seen in Fig. D.3. This has led some to argue that the ability to measure δ is independent, to some extent, of the value of $\sin^2(2\theta_{13})$. We will see that there are regions of $\sin^2(2\theta_{13})$ in which the probability of measurement is flat. We will also see that there can be peaks and dips in the probability as a function of $\sin^2(2\theta_{13})$ due to the complex relationship between CP-violating effects and matter effects.

In order to take this relationship into account, we use the following measure of our ability to measure CP violation: the fraction of possible δ values for which there is a three standard deviation demonstration of CP violation, that is, that δ is neither zero nor π for both mass orderings. Of course, this fraction can never be 100%, since there will always be some range of δ values very close to zero or π. A rough way to convert this measure into a one standard deviation measure of δ is that a small, but non-zero fraction corresponds to 30 degrees, a 25% fraction to 22.5 degrees, a 50% fraction to 15 degrees, and so on.

D.5.2: Simulation Results: Neither NOνA nor T2K can demonstrate CP violation even at the two standard deviation level with six years of running without an enhanced proton source. However, both experiments gain some ability with their proposed proton drivers. This is shown in Fig. D.17, in which both experiments are assumed to have run three years each on neutrinos and antineutrinos and the T2K detector is assumed to be SuperKamiokande. T2K has a broader reach than NOνA in $\sin^2(2\theta_{13})$, but saturates at a lower fraction of δ due to its inability to resolve the mass hierarchy.

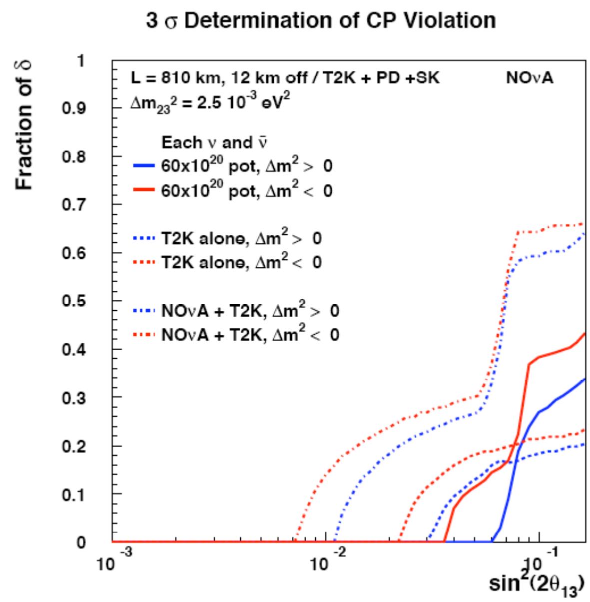

Fig. D.17: The fraction of δ values for which CP violation can be demonstrated at three standard deviations. A three year run on each of neutrinos and antineutrinos is assumed for NOνA with the Proton Driver and for T2K with an enhanced proton source and SuperKamiokande as the detector.

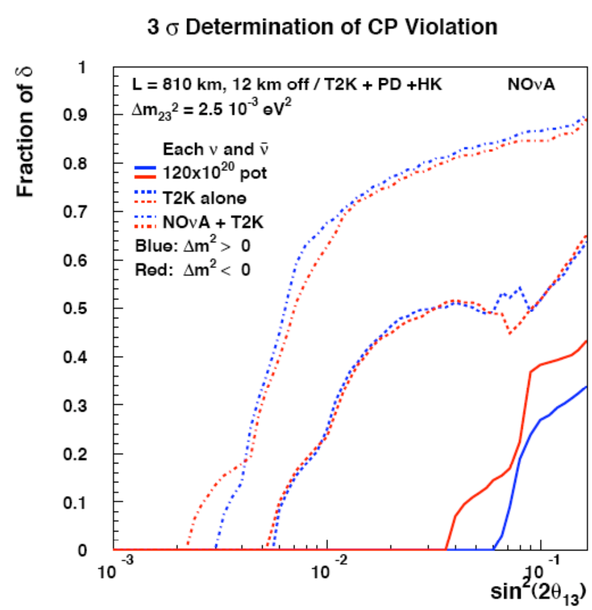

Fig. D.18: The same as Fig D.17 except that HyperKamiokande is assumed to be the T2K detector.

Combining measurements from both experiments gives a large gain in both the breadth and precision of the measurement. The sharp rise

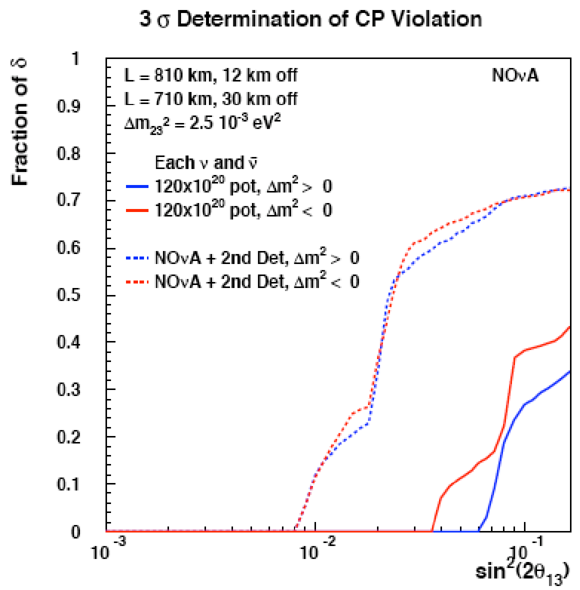

Fig. D.19: The fraction of δ values for which CP violation can be demonstrated at three standard deviations for NOνA with the Proton Driver and combined with an additional detector on the NuMI beam line, as discussed in the text.

around $\sin^2(2\theta_{13}) = 0.05$ is due to the resolution of the mass hierarchy, as discussed in Section D.4.3 and seen in Fig. D.13.

Fig. D.18 shows the same information as Fig. D.17, except that HyperKamiokande is assumed to be the T2K detector. The twenty-fold increase in mass gives it high statistical precision. The role of NOνA is to resolve the mass hierarchy so that the precision can be used, as was discussed in the opening section of this appendix.

Finally, Fig. D.19 addresses the CP violation measurements that could be made by a combination of NOνA and the additional detector on the NuMI beamline, running at the second oscillation maximum, that was suggested in Section D.4.3 to resolve the mass hierarchy in the case of small values of $\sin^2(2\theta_{13})$. This figure shows that there is also a good capability for measuring CP violation at these $\sin^2(2\theta_{13})$ values.

Appendix D References

[1]T2K Letter of Intent, January, 2003. http://neutrino.kek.jp/jhfnu/.

[2] See, for example, M. Mezzetto, http://axpd24.pd.infn.it/NO-VE/index-of-transparencies.html

[3] M. Ishitsuka, http://www-sk.icrr.u-tokyo.ac.jp/noon2004/.

[4] CHOOZ Collaboration, M. Apollonio et al., *Phys. Lett B* **466**, 415 (1999).